FREQUENCY BANDED WAVE CHARACTERISTIC OBSERVED BY GPS BUOYS OFF THE PACIFIC COAST OF JAPAN

K. Seki [1], H. Kawai [1], K. Kawaguchi [1] and T. Inomata [1]

ABSTRACT: Fifteen GPS buoys, which measure the vertical motion of the buoy due to waves and tides by the RTK-GPS technology, are moored at a spot of 100-400 m in water depth and within 10-20 km from the shoreline around the Japanese coast. They are the newest equipment on the Nationwide Ocean Wave Information Network for Port and Harbours (NOWPHAS). This study conducted the statistical analysis on four frequency banded wave components (short-period wind wave, long-period wind wave, swell and infra-gravity wave) acquired by the GPS buoys and their nearby coastal wave gauges. A high correlation was found in these frequency banded wave heights, in particular two long period components between a GPS buoy and its nearby coastal wave gauge. The correlation between the long period wave component heights and the significant wave height at the GPS buoys is high, while the ratio of the swell height to the significant wave height varies with the incident wave direction and the meteorological conditions. The swell direction sometimes differs from the wind wave direction. The ratio of the swell height to the significant wave height in the entire band varies around the time when the significant wave height reached its maximum during the 2009 Typhoon Melor event.

Keywords: NOWPHAS, GPS buoy, frequency banded wave component

INTRODUCTION

Wave conditions have been observed around Japan through the Nationwide Ocean Wave information network for Port and HArbourS (hereinafter, NOWPHAS) since 1970 (Nagai et al. 1994). The number of the stations with seabed ultrasonic wave gauges (hereinafter, coastal wave gauge), which measure the water surface elevation every 0.5 s on a 20-60 m deep seabed and normally within 3 km from the shoreline, was 61 in 2011. The NOWPHAS data is useful for the verification of a long-term trend in wave statistics (Seki et al. 2012).

The installation water depth of coastal wave gauges is too shallow to monitor deepwater waves; therefore, wave buoys are also applied in NOWPHAS. The newest equipment is a GPS buoy, which measures the altitude, latitude and longitude of the GPS receiver on the top of the buoy each second by using the RTK-GPS technology (Kato et al., 2001; Shimizu et al., 2006) at a spot of 100-400 m in water depth and normally within 10-20 km from the shoreline. The monthly-mean deepwater wave characteristics on GPS buoys were compared with shallow-water ones on their geometrically adjacent coastal wave gauges (Kawai et al. 2013). This study examined the statistics on frequency banded wave components.

WAVE STASTIONS AND DATA ANALYSIS ON NOWPHAS

Wave Stations

The Ports and Harbours Bureau of the Ministry of Land, Infrastructure, Transport and Tourism, and its associated agencies, including the Port and Airport Research Institute (PARI), have been conducting wave observations on the Japanese coast through the Nationwide Ocean Wave information network for Ports and HArbourS (NOWPHAS), since 1970. Real-time data acquisitions, processing, dissemination through the Internet are currently operated on the system. Figure 1 shows the increase in the station with coastal wave gauges, where the number of the stations has reached 61 in 2011. The number of GPS buys increased to 15 until 2011. All the wave stations are shown in Fig. 2.
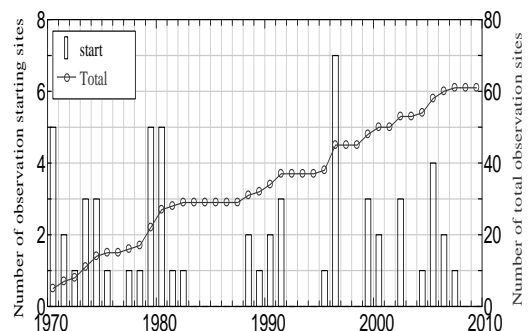

Fig. 1 Transition of the number of stations

[1] Marine Information Field, Port and Airport Research Institute, 3-1-1 Nagase, Yokosuka, Kanagawa, 239-0826, JAPAN
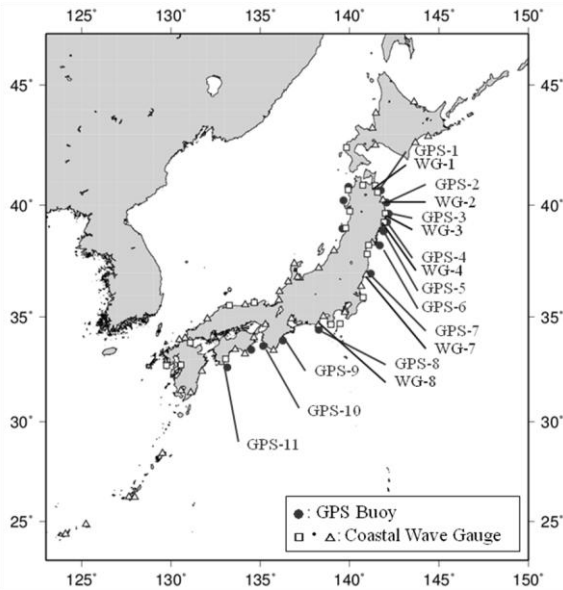
Fig. 2 Wave observation stations in NOWPHAS

Table 1. Division of frequency bands

Band	Period	Frequency
f1	30s <	0.003Hz >
f2	15 - 30s	0.039 - 0.063Hz
f3	10 - 15s	0.070 - 0.094Hz
f4	8 - 10s	0.102 - 0.125Hz
f5	6 - 8s	0.133 - 0.164Hz
f6	6s >	0.172Hz <

Table 2 Water depth and coordinates of the presented stations

No.	Name	Depth [m]	Latitude °	Latitude ′	Latitude ″	Longitude °	Longitude ′	Longitude ″
GPS-1	East Aomori	87	40	38	0	141	45	0
GPS-2	North Iwate	125	40	7	0	142	4	0
GPS-3	Central Iwate	200	39	37	38	142	11	12
GPS-4	South Iwate	204	39	15	31	142	5	49
GPS-5	North Miyagi	160	38	51	28	141	53	40
GPS-6	Central Miyagi	144	38	13	57	141	41	1
GPS-7	Fukushima	137	36	58	17	141	11	8
GPS-8	Shizuoka-Omaezaki	120	34	24	12	138	16	30
GPS-9	Mie-Owase	210	33	54	8	136	15	34
GPS-10	Southwest-Wakayama	201	33	38	32	135	9	24
GPS-11	West Kochi	309	32	37	52	133	9	21
WG-1	Hachinohe	27.7	40	33	39	141	34	6
WG-2	Kuji	49.5	40	13	4	141	51	36
WG-3	Miyako	24.2	39	38	22	141	59	9
WG-4	Kamaishi	49.8	39	15	54	141	56	6
WG-7	Onahama	23.8	36	55	4	140	55	18
WG-8	Omaezaki	22.8	34	37	17	138	15	33

Data Analysis

In frequency banded wave analysis on NOWPHAS, wave frequency spectrum is divided in to 6 frequency bands, from the lowest frequency band f1 (corresponding period > 30 s) to the highest frequency band f6 (<6 s), in Table 1 (Shimizu et al. 2006). Frequency banded wave heights are calculated by integrating wave frequency

spectrum from lower to higher frequency thresholds. The principal wave directions are estimated for the intermediate bands of f2-f5.

This research, however, excluded the high frequency bands f5 and f6, because their frequency bands are near to the natural period of the vertical motion of the GPS buoys. The stations focused here are 11 GPS buys and 6 coastal wave gauges among the stations in Fig.2 and these station names, installation water depths and coordinates are listed as of those locations are shown in Table 2, where GPS-X and WG-X indicate a GPS buoy and a coastal wave gauge, respectively.

CORRELATION ON FREQUENCY BANDED WAVE STATISTICS

Pairs of Wave Statistics

This research selected 6 pairs of a GPS buoy and its nearby coastal wave gauge and conducted the correlation analysis on the frequency banded wave statistics in each pair. Table 3 shows the distance and azimuth from the GPS buoys to the coastal wave gauge. Hence, the distances are all less than 30 km.

Figure 3 chooses GPS-4 and WG-4 as one of the pairs and shows the locations of the stations with their surrounding bathymetry.

Table 3 Pairs of GPS buoys and coastal wave gauges

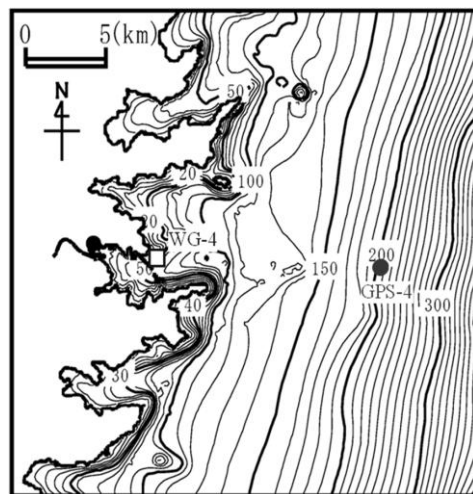| GPS buoy No.	Depth [m]	Coastal wave gauge No.	Depth [m]	Distance [km]	Azimuth
GPS-1	87	WG-1	27.7	17.5	ENE
GPS-2	125	WG-2	49.5	20.9	ESE
GPS-3	200	WG-3	24.2	17.3	E
GPS-4	204	WG-4	49.8	13.9	E
GPS-7	137	WG-7	23.8	24.2	ENE
GPS-8	120	WG-8	22.8	24.2	S

Fig. 3 Bathymetry around GPS-4 and WG-4

Wave Height Ratio between Wave Stations

Figure 4 shows the correlation of the frequency banded wave heights between GPS-4 and WG-4 for the wave directions of NE and S on GPS-4. The ratio (WG-4/GPS-4) for NE is larger than that for S, in all the frequency bands. The bathymetry surrounding WG-4 might shelter from ocean waves, in particular those from S, and introduce such difference in the ratio.
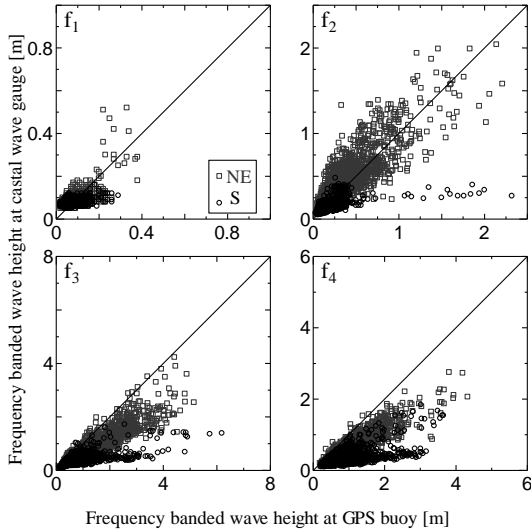
Table 4 shows the frequency banded wave height ratio (WG-X/GPS-X) for major wave directions including the azimuth toward GPS-X from WG-X, in all the pairs in Table 3, where the cells with the ratios higher than 1.5 are highlighted. The ratios for low frequency bands f1 and f2 (infra-gravity waves and swell) are mostly larger or near 1, except for the pair of GPS-3 and WG-3. Figure 6 shows that the bathymetry around WG-3 can shelter ocean waves much more than that around WG-3 in Fig.3.

Fig. 4 Comparison of the frequency banded wave heights between GPS-4 and WG-4

Figure 5 shows the variation of the frequency banded wave height ratios (WG-4/GPS-4) with the wave direction on GPS-4 in each frequency band. Hence, $H_{1/3}$ and $T_{1/3}$ indicate the ratios of the significant wave height and period for the entire frequency band. The ratios for the low frequency bands f1 and f2 are much larger than those for the other bands. The variation of the ratios for f1 and f2 with the wave directions are narrower than those for the others. These results could reveal that the low frequency wave components are diffracted more than high frequency ones.
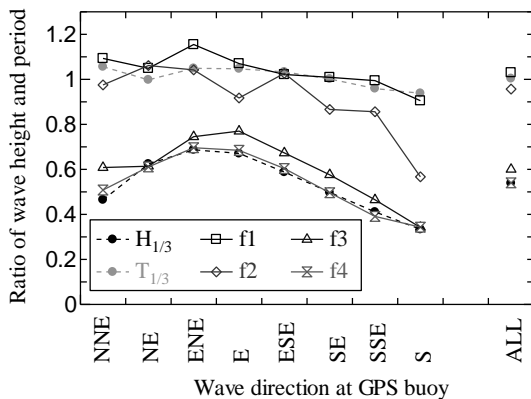
Table 4 Frequency banded wave height ratios

| Set	Wave direction at GPS buoy	$H_{1/3}$	f1	f2	f3	f4
GPS-1	NE	0.780	1.221	1.727	0.969	0.790
vs	ENE	0.832	1.321	1.876	0.944	0.793
WG-1	E	0.737	1.059	1.514	0.915	0.747
GPS-2	E	0.834	0.792	1.170	0.956	0.843
vs	ESE	0.820	0.739	1.425	0.952	0.823
WG-2	SE	0.779	0.716	1.259	0.907	0.796
GPS-3	ENE	0.434	0.584	0.627	0.406	0.417
vs	E	0.331	0.460	0.332	0.300	0.277
WG-3	ESE	0.270	0.452	0.398	0.286	0.207
GPS-4	ENE	0.687	1.155	1.042	0.745	0.696
vs	E	0.671	1.070	0.917	0.770	0.685
WG-4	ESE	0.588	1.022	1.027	0.673	0.604
GPS-7	NE	0.671	0.948	1.097	0.771	0.677
vs	ENE	0.722	0.979	1.265	0.859	0.726
WG-7	E	0.747	1.031	1.531	0.854	0.747
GPS-8	SSE	0.753	1.057	1.807	0.980	0.730
vs	S	0.664	0.898	1.685	0.850	0.656
WG-8	SSW	0.572	0.828	1.296	0.612	0.575
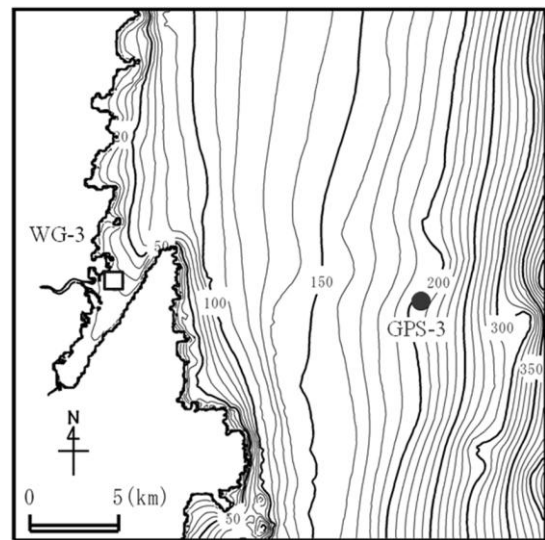
Fig. 6 Bathymetry around GPS-3 and WG-3

Wave Height Ratio between Frequency Bands and Entire Band

Figure 7 compares the wave height H1 in frequency band f1 with the significant wave height $H_{1/3}$ in entire frequency band, for all the wave directions and ESE alone, on GPS-4. Solid lines are the linear regression lines (H1=$aH_{1/3}$), and the dotted lines are the square regression line (H1=$aH_{1/3}^2$). A high correlation was

Fig. 5 Variations of the frequency banded wave heights and the significant wave height and period ratios

obtained between $H_{1/3}$ and H1, not only for ESE but also for all the directions.

(a) All direction   (b) ESE
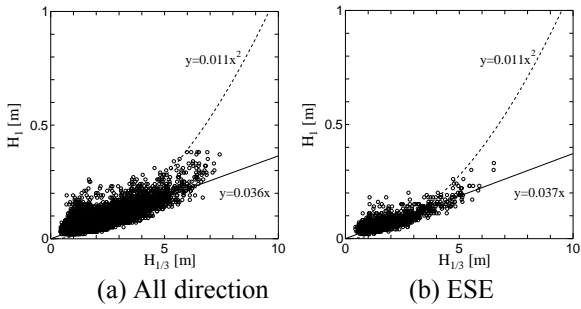
Fig. 7 Comparison of the wave height H1 with $H_{1/3}$ on GPS-4

Figure 8 compares the wave height H2 in frequency band f2 with $H_{1/3}$. The correlation between $H_{1/3}$ and H2 is much lower than that between $H_{1/3}$ and H1, not only for ESE but also for all the directions. The comparison with Fig. 7 reveals that H2 varies with direction much more than H1.
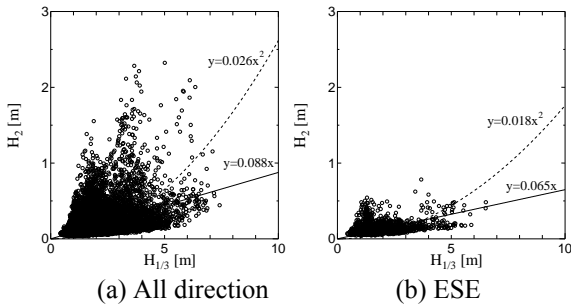

(a) All direction   (b) ESE

Fig. 8 Comparison of the wave height H2 with $H_{1/3}$ on GPS-4

Table 5 shows the regression coefficient *a* and correlation coefficient *r* on 11 GPS buoys. The correlation coefficient in the linear regression is higher than that in the square one. The regression coefficient in linear regression is around 0.4.

Table 5. Regression and correlation coefficient

No.	f1		f2	
	a	*r*	*a*	*r*
GPS-1	0.040	0.678	0.072	0.207
GPS-2	0.044	0.373	0.074	0.229
GPS-3	0.034	0.642	0.085	0.219
GPS-4	0.036	0.622	0.088	0.204
GPS-5	0.035	0.564	0.088	0.213
GPS-6	0.036	0.709	0.082	0.198
GPS-7	0.037	0.544	0.077	0.190
GPS-8	0.041	0.634	0.069	0.146
GPS-9	0.041	0.591	0.101	0.234
GPS-10	0.036	0.384	0.043	0.090
GPS-11	0.042	0.601	0.089	0.246

DEEPWATER WAVE CHARACTERISTIC DUARING TYHPOON PASSAGE

In this chapter, we will discuss on deepwater frequency banded wave statistics during the passage of Typhoon Choi-wan (No. 0914) and Melor (No. 0918) attacked for Japanese coast in autumn 2004. Figure 9 shows the tracks of these typhoons, and Fig. 10 enlarged the track of Typhoon Melor. GPS-9 recorded the maximum significant wave height on NOWPHAS (15.14 m, 14.4s) during Typhoon Melor (Kawai et al. 2011).
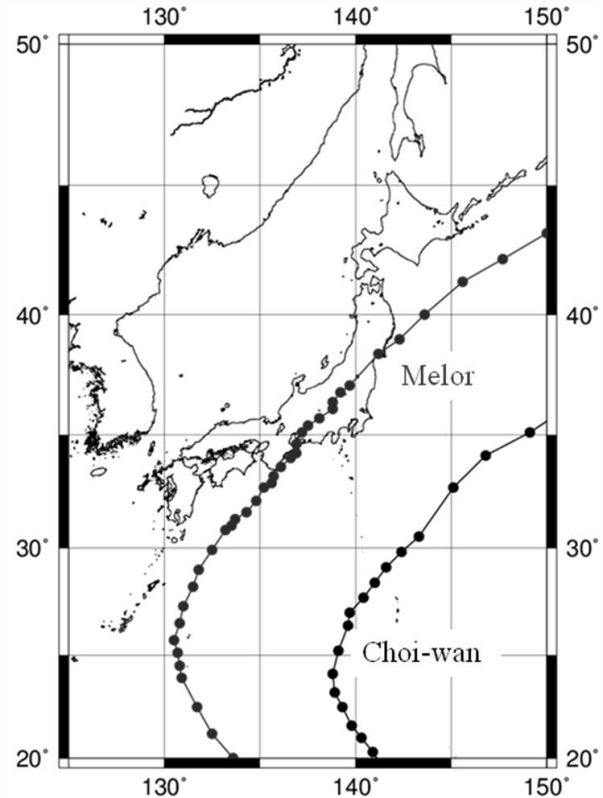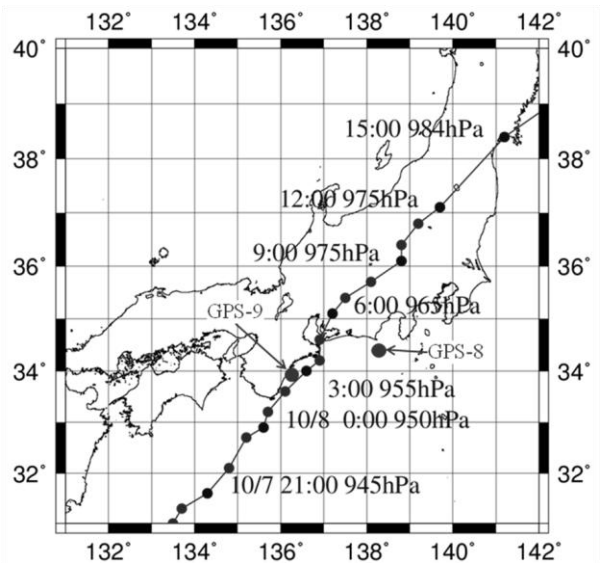

Fig. 9 Tracks of Typhoon Choi-wan and Melor

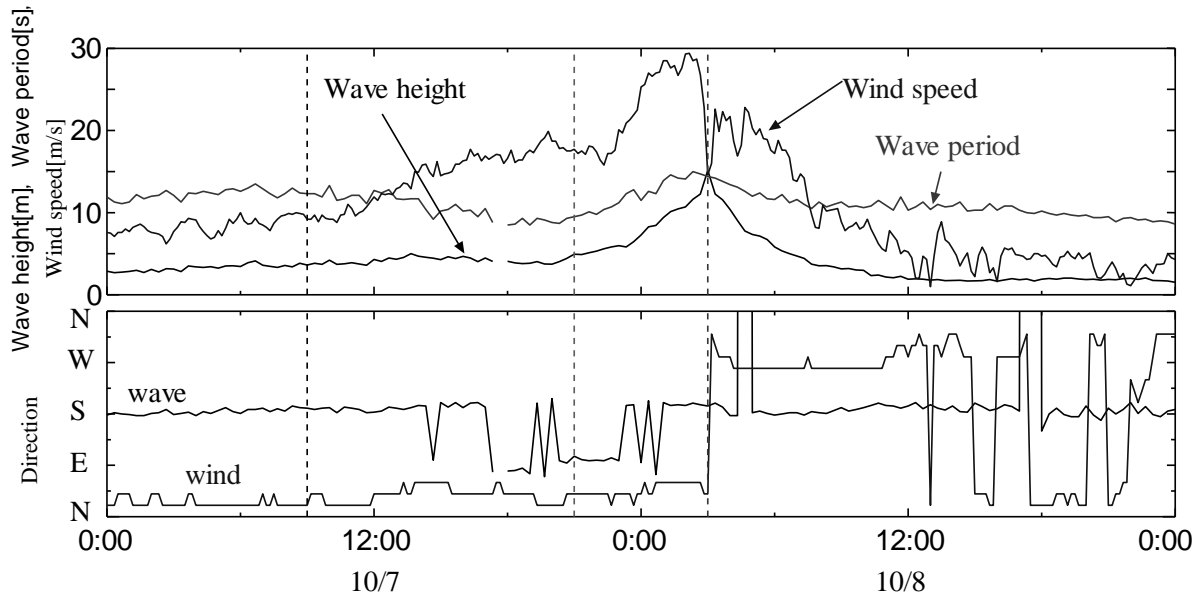Fig. 10. Enlarged track of Typhoon Melor (JST)

Fig. 11 Timeline of the significant wave height and period, 10-min-averaged wind speed, wave and wind directions on GPS-9 on October 7 and 8, 2009 in JST.
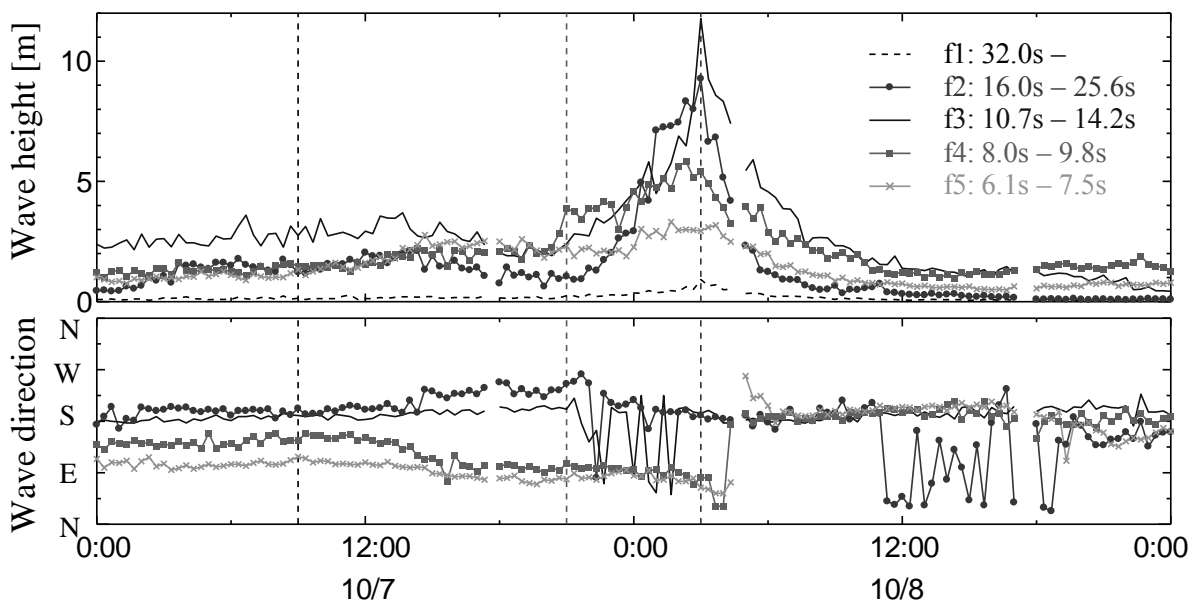

Fig. 12 Timeline of the frequency banded wave height and direction on GPS-9 on October 7 and 8, 2009 in JST.

Variation of Frequency Banded Wave Height and Direction with Time

Figure 11 shows the timeline of the significant wave height and period, 10-min-averaged wind speed, wave and wind directions on GPS-9 on October 7 and 8, 2009, in JST (GMT+9h), when the Typhoon Melor passed by the station. The significant wave height increased remarkably from 21:00, October 7, when the typhoon center was located at 350 km away from the observation station, and then reached the maximum at 2:40, October 8. In contrast, the significant wave period decreased and wave direction changed from S to E at 18:00, October 7. Such variations mean that that east strong wind in the

typhoon front generated wind wave (short period wave) quickly.

Figure 12 shows the timeline of the frequency banded wave height and wave direction during the same term as Fig.11. The wave height in high frequency band f4 began to increase earlier than the low frequency bands f2 and f3. Such difference in time can be explained by that the group velocity (around 28 km/h) was slower than the typhoon forwarding speed (around 50 km/h). The wave direction in low frequency bands f2 and f3, did not change so much, while that in the high frequency bands f4 and f5 changed from S to E to follow the change in the wind direction.
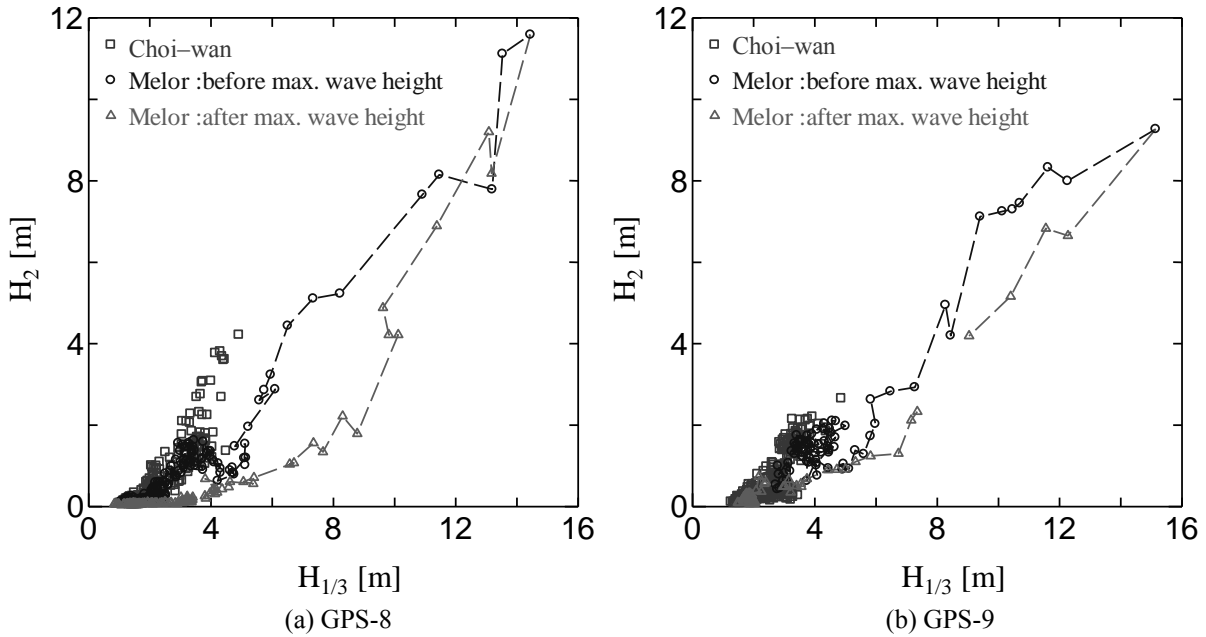
(a) GPS-8

(b) GPS-9

Fig. 13 Comparison the frequency banded wave height H2 with the significant wave height on GPS-8 and GPS-9

Variation of the Wave Height Ratio (H2/$H_{1/3}$) with Time

Figure 13 compares the frequency banded wave height H2 in frequency band f2 with the significant wave height $H_{1/3}$ on GPS-8 and GPS-9 during the passage of Typhoon Choi-wan and Melor. Typhoon Choi-wan did not made landfall on the Japanese coast, and consequently the maximum significant wave height was around 5m.

The data plotted in the figure were obtained when the significant wave height was less than 4 m and the typhoon center were located at 25-30 degree north in latitude.

The plots for Typhoon Melor shifted to right side of the figure after the maximum significant wave height. It means that the wave height ration (H2/$H_{1/3}$) became small while the significant wave height decreased.

Variation in Deepwater Wave Power Spectrum during the Storm

Figure 14 shows the power spectrum of deepwater wave on GPS-9, which was determined by FFT (fast Fourier transform) method. The Colors of the line in this figure correspond to the times (9:00 October 7; 21:00 October 7; and 3:00 October 8) for the vertical dotted lines, in Fig.11 and 12.

The wave energy in high frequency bands f4-f6 increased earlier than low frequency bands f2 and f3, as shown in Fig. 12.
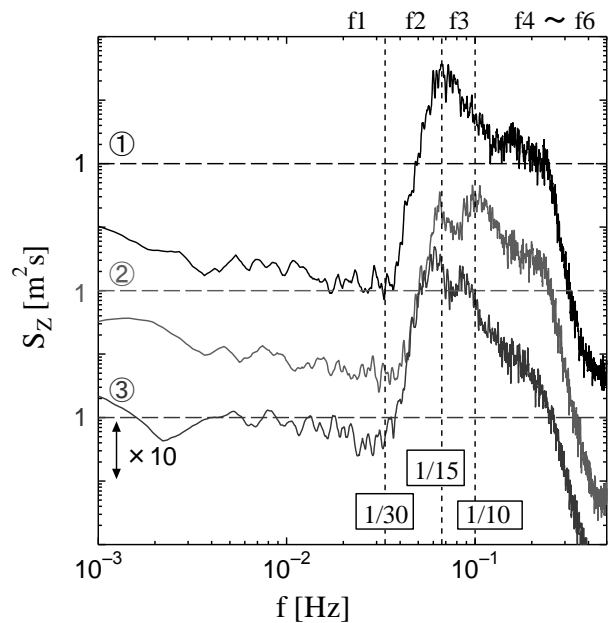

Fig. 14 Power spectrum of deepwater waves on GPS-9

CONCLUSION

This research determined the deepwater and shallow-water frequency banded wave statistics on GPS buoys and coastal wave gauges. The conclusions are as follows;

(1) A high correlation was found in the frequency banded wave heights between GPS buoy and its nearby coastal gauge.

(2) The wave height ratio (WG/GPS) is mostly larger or near 1 in low frequency band.

(3) The regression coefficient between the significant wave height and the infra-gravity wave (frequency band f1) height is around 0.4 for linear regression.

(4) The swell (frequency band f2) direction sometimes differs from the wind wave direction. The ratio of the swell height to the significant wave height in the entire band varies around the time when the significant wave height reached its maximum during the 2009 Typhoon Melor event.

In further research, the physical process that is generation and transformation of infra-gravity wave and swell should be discussed by using the numerical models.

ACKNOWLEDGEMENTS

REFERENCES

Kato, T., Terada, Y., Kinoshita, M., Kakimoto, H., Issiki, H., Moriguchi, T., Takada, M., Tanno, T., Kanzaki, M. and Johnson, J. (2001). A new tsunami monitoring system using RTK-GPS. ITS 2001 Proc. Ses. 5. No. 5-12. Austrasia: 645-651.

Kawai, H., Satoh, M., Kawaguchi, K. and Seki, K. (2011). Annual report on nationwide wave information network for port and harbours (NOWPHAS2009). Technical note of the port and airport research institute. No1226.

Kawai, H., Seki, K., Kawaguchi, K. and Inomata, T. (2013). Deepwater wave characteristics around Japan observed by NOWPHAS GPS buoy network. 23nd Int. Offshore and Polar Engineering Conf. Anchorage. USA.

Nagai, T., Sugahara, K., Hashimoto, N., Asai, T., Higashiyama, S. and Toda, K. (1994). Introduction of Japanese NOWPHAS system and its recent topics. Proc. Int. Conf. on Hydro-Technical Engineering for Port and Habour. PHRI. Japan: 67-82.

Seki, K., Kawai, H., Kawaguchi, K. and Inomata, T. (2012). Long-term trend of wave characteristics on Japanese coast based on NOWPHAS data. 22nd Int. Offshore and Polar Engineering Conf. Rhodes. Greece: 685-692.

Shimizu, K., Nagai, T., Satomi, S., Lee, J. H., Kudaka, M. and Fujita T. (2006). Development of the deep-sea GPS buoy wave data processing system. Proc. of Techno-Ocean 2006. Japan: No.27.